JOURNAL OF THE KOREAN ASTRONOMICAL SOCIETY
31: 67 ~ 74, 1998

THE VI CCD PHOTOMETRY OF THE GLOBULAR CLUSTER M22*

CHO, DONG HWAN [1], **LEE, SEE-WOO** [1] **AND SUNG, HWANKYUNG** [2]
[1] Department of Astronomy, Seoul National University
[2] Research Institute for Basic Sciences, Seoul National University
(Received Mar. 31, 1998; Accepted Apr. 15, 1998)

ABSTRACT

The VI CCD photometry is made for stars in the globular cluster M22 down to $V \approx 19^m$, $I \approx 18^m$. In the color-magnitude diagram (CMD), red giant branch (RGB), asymtotic giant branch (AGB) and blue horizontal branch (BHB) are well defined. The luminosity functions (LF) of RGB, AGB and BHB stars are derived, discussing deficient gaps and bumps in the CMD. The anomalously wide RGB seen in the BV photometric system is found to disappear in the VI photometric system.

Key Words : techniques: photometry — globular clusters: individual (M22) — color-magnitude diagram — stars: luminosity function

I. INTRODUCTION

The globular cluster, M22 ($\alpha_{2000} = 18^h\ 36^m\ 24.2^s$, $\delta_{2000} = -23°\ 54'\ 12''$; $l = 9.9°$, $b = -7.6°$) is located at low galactic latitude in the central direction to the Galaxy. As $R_\odot = 3.0$ kpc, M22 is a fourth closest galactic globular cluster to us, following M4 (1.73 kpc), NGC 6397 (2.2 kpc) and NGC 6544 (2.4 kpc). In the direction to M22 the Sagittarius spiral arm is located, and behind it the background of the Galactic bulge is seen. Therefore, the cluster members fainter than $V \approx 15^m$ are severly contaminated by many field stars and particularly by the bulge stars.

The core radius (r_c), half-mass radius(r_h) and tidal radius (r_t) are respectively, $r_c = 1.42'$, $r_h = 3.26'$ and $r_t = 33'$ (Peterson & King 1975). The total mass was estimated to be about $5 \times 10^5 M_\odot$ by Pryor & Meylan (1993), and so M22 is relatively a large globular cluster in the Milky Way. As shown in Table 1, the interstellar reddening of M22 has been measured by many investigators using various methods. Their values range from $E(B-V) = 0.24^m$ to 0.42^m, implying a possible differential reddening across the cluster. Actually Bates, Gilheany & Wood (1991) reported that the south-eastern part of M22 reveals systematically larger reddening as compared with other regions.

There have been found many peculiar objects in M22. The most of them were examined spectroscopically and bright objects of them were also observed photometrically. These include peculiar stars such as two Ba stars (Mallia 1976), three CH stars (Hesser, Hartwick & McClure 1977, Hesser & Harris 1979), a sdO star (Glaspey et al. 1985) and some sdB stars (Moehler et al. 1995), and special objects such as four dim X-ray sources (Hertz & Grindlay 1983) and a planetary nebular IRAS 18333–2357 (Gillett et al. 1989). Spectroscopic studies about M22 have been mainly devoted to metallicity determination as shown in Table 2. From the study of CH, CN and Ca abundances for about 100 giant stars in M22, Norris & Freeman (1983) reported that M22 shows the metallicity inhomogeneity similar to ω Centauri. This effect is also seen in Table 2, in which spectroscopic metal abundances range from [Fe/H] = −1.94 to −1.48, and their mean value weighted by the observed number of stars is <[Fe/H]> = −1.68. The largest value was obtained most recently by Carretta & Gratton (1997). This large difference (~ 0.5 dex) in metallicity is likely to be attributed to the intrinsic dispersion of metallicity like ω Centauri (Luck 1991) rather than the observational uncertainty.

Since the first observation by Arp & Melbourne (1959), M22 has been investigated photometrically by many authors, showing a wide RGB in the [V vs. $(B-V)$] CMDs (Alcaino 1977; Alcaino & Liller 1983; Cudworth 1986;

* This work was supported by Ministry of Education, Basic Science Research Institute, Grant No. BSRI-97-5411.

Table. 1. Measured values of $E(B-V)$

$E(B-V)$	Method	Author
0.39^m	Measurement of integrated light ($uvby\beta$)	Johnson & McNamara (1969)
0.25^m	Use of early type stars of the cluster	Eggen (1972)
0.35^m	Measurement of integrated light (UBV)	Harris & van den Bergh (1974)
0.24^m	Photometry of $ubvy\beta$	Crawford & Barnes (1975)
0.40^m	Photometry of $ubvy\beta$	Philip & Goodman (1975)
0.32^m	Photometry of $ubvy\beta$	Hesser (1976)
0.32^m	Measurement of integrated light	Zinn (1980)
0.34^m	Theoritical calculation	Reed et al. (1988)
0.42^m	Comparison of the temperatures of HB stars	Crocker (1988)

Table. 2. Measured values of [Fe/H]

[Fe/H]	Method (Number of stars)	Author
−1.70	ΔS method (6)	Butler (1974)
−2.00	Washington photometry (5)	Canterna (1975)
−1.60	Spectroscopic study (3)	Manduca & Bell (1978)
−1.94	Spectroscopic study by high dispersion echelle (4)	Peterson (1980)
−1.78	Spectroscopic study by high dispersion echelle (3)	Cohen (1981)
−1.94	Spectroscopic study by high dispersion echelle (3)	Gratton (1982)
−1.67	Spectroscopic study by high dispersion echelle (6)	Pilachowski et al. (1982)
−1.60	High dispersion spectroscopic study (2)	Wallerstein et al. (1987)
−1.56	Spectroscopic study by high dispersion echelle (3)	Gratton & Ortolani (1989)
−1.54	High dispersion spectroscopic study (10)	Lehnert et al. (1991)
−1.67	Spectroscopic study by high dispersion echelle (7)	Brown & Wallerstein (1992)
−1.75	Spectroscopic study (10)	Minniti (1995)
−1.48	Reanalysis of high dispersion echelle spectra (3)	Carretta & Gratton (1997)

Peterson & Cudworth 1994), of which the peculiar phenomenon has been well known in ω Centauri (Cannon & Stewart 1981).

In order to examine whether this wide RGB appears also in the CMD obtained by the VI system, we made the VI CCD photometry down to $V \approx 19^m$ and $I \approx 18^m$. The observations and reduction of data are presented in section II, and the characteristics of the CMD are discussed in section III. The LFs of each branch stars are examined in section IV, presenting the conclusion in the last section.

II. OBSERVATIONS AND DATA REDUCTION

The observations were made by one of us (H.S.) with the 1-m telescope ($f/8$) at the Siding Spring Observatory of Australian National University on August 25, 1995. The Tektronics 2048 × 2048 CCD camera was used as a detector. The gain of the CCD was set to 2 e^-/ADU. The read-out noise was ~ 43.8 e^- which was estimated from the standard deviation of bias frames. The scale is $0.61''/pixel$, covering a field of $20.8'$ on a side. Exposure times were 10 seconds and 100 seconds with V-filter and 5 seconds and 50 seconds with I-filter. During exposure, the seeing was $2.0'' \sim 2.3''$.

The actual photometry was performed within $12'$ from the image center of frame as seen in Figure 1. The center of the cluster was crowded and shifted slightly from image center, and hence measurements were performed in the regions between $4'$ and $12.6'$ from the adopted cluster center in the case of long exposures, and between $2.2'$ and $4'$ in the case of short exposures. In order to obtain correct magnitudes of saturated stars in the long exposure frames, we applied correction to their measured magnitudes on the basis of magnitudes obtained from the unsaturated short exposure frames.

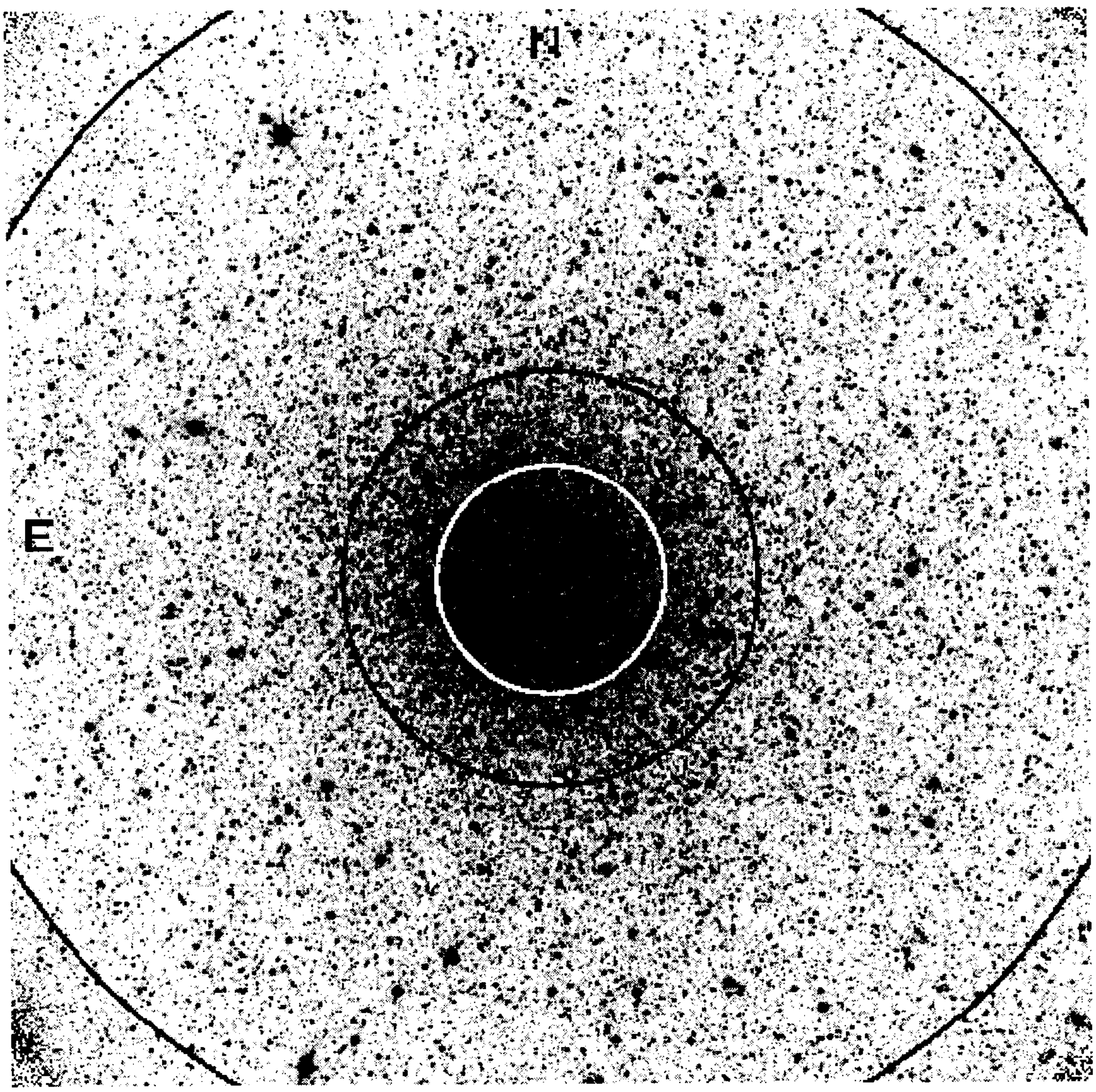

Fig. 1. The image of long exposure frame of M22 in V-band. The radius of the first white ring is $2.2'$ from the adopted cluster center and that of the second black ring is $4'$ from the adopted cluster center. The outer ring denotes a photometric boundary for measurements, and its radius is $12'$ from the frame center. The size of the frame is $20.8' \times 20.8'$.

Pre-processing including trimming, bias subtraction, flat fielding and cosmic ray rejection in each frame were done using IRAF/CCDRED package. Instrumental magnitudes of stars in each frame were determined from the IRAF version of DAOPHOT (Stetson, Davis & Crabtree 1990). To achieve the better photometric accuracy, DAOFIND routine was run only once by setting the signal detection threshhold at 3σ. After selecting about 50 stars which are well separated from neighbor stars and have high image quality in each frame, a point-spread function (PSF) was derived from 45 $\sim$ 50 stars which fit a quadratic function very well and do not leave any residuals after several iterations of the PSF routine. After obtainning instrumental magnitudes, in order to reject ghost stars, we rejected stars with PSF error larger than 0.1^m and sharpness smaller than -1.0.

To apply aperture corrections, we selected about 200 stars with good image quality over a whole region of each frame. After subtracting neighbor stars around each selected stars which could affect the sky brightness, we did the aperture photometry with the same aperture size as used for standard stars. Then, we derived differences between instrumental magnitudes obtained by aperture photometry and PSF photometry for each star. These differences had a linear variation with distance from the image center, and the degrees of variations were different frame to

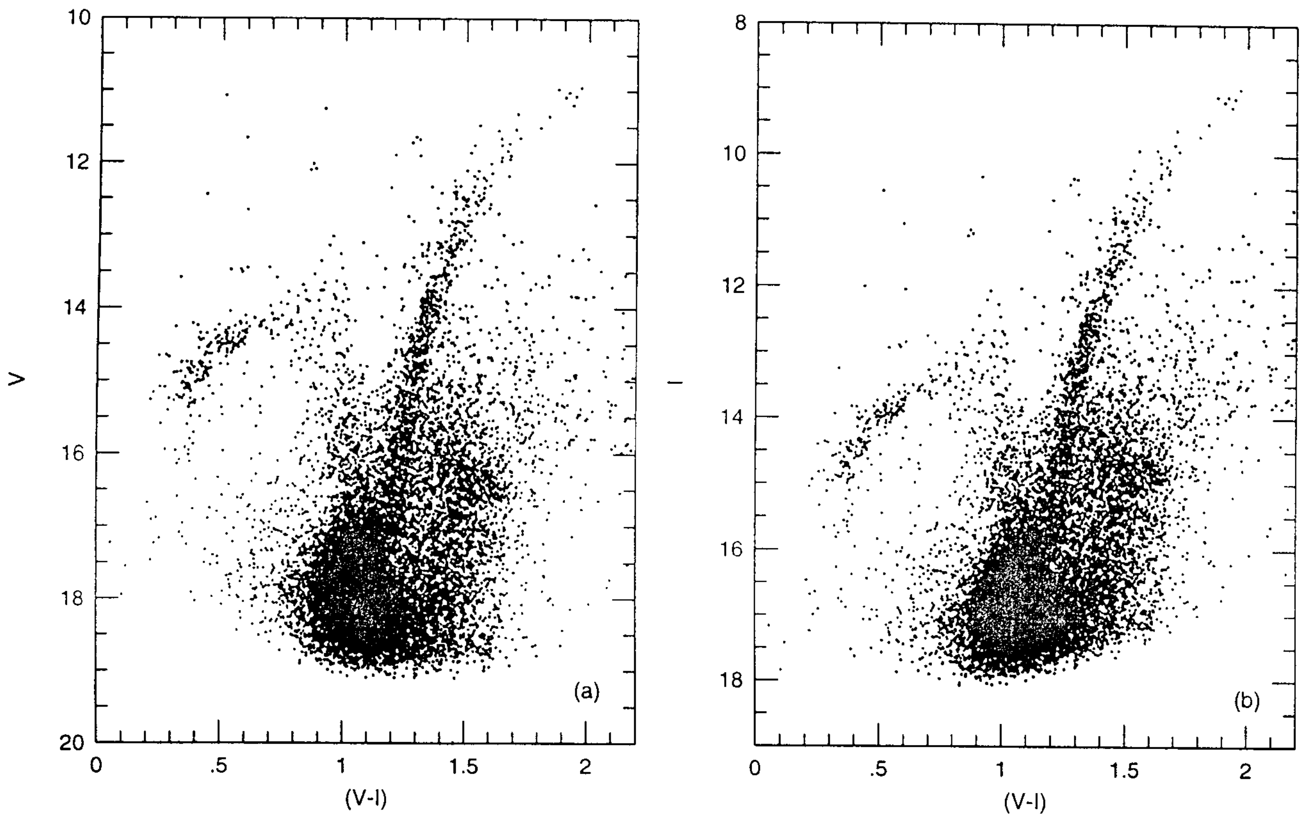

Fig. 2. The CMDs for 13,536 stars in the observed region of M22.

frame. This relation was applied to correct PSF instrumental magnitudes obtained in each frame.

The instrumental system can be converted to the standard system by transformation equations. Color coefficients in the equations were determined using many standard stars given by Landolt (1992) and given in many open clusters. Zero points were determined from 15 photoelectric $UBVRI$ standard stars given by Alcaino et al. (1988). The derived transformation equations are as follow:

$$V = v - 0.027(\pm 0.010)(V - I) - 3.251(\pm 0.037)$$

$$I = i + 0.051(\pm 0.013)(V - I) - 3.311(\pm 0.033)$$

where V and I are standard magnitudes, and v and i are instrumental magnitudes applied aperture corrections. From the above equations, we determined magnitudes and colors for total 13,536 stars within the observed region of M22. Obsevational errors are $\varepsilon(V) = 0.01^m$, $\varepsilon(V - I) = 0.02^m$ down to $V = 16^m$, and $\varepsilon(V) = 0.10^m$, $\varepsilon(V - I) = 0.14^m$ at $V = 19^m$.

III. COLOR-MAGNITUDE DIAGRAM

Using the data of V, I and $(V - I)$, two CMDs were derived in Figure 2. Here the faint limiting magnitudes are $V \approx 19^m$, $I \approx 18^m$, which are fainter by more than one magnitude than the main-sequence turnoff point ($V \approx 17.8^m$, $I \approx 16.7^m$). In the CMDs, the observed ranges of magnitudes are $\Delta V \approx 8^m$ and $\Delta I \approx 9^m$. Although the cluster member stars fainter than $V = 15.5^m$ are severly contaminated by the Galactic bulge stars, the RGB is clearly well defined from $V = 11^m$ to 16.5^m. And its intrinsic width $\Delta(V - I) \approx 0.06^m$ for $V < 15^m$ which is only one third of the RGB width, $\Delta(B - V) \approx 0.18^m$ obtained from the BV system (Cudworth 1986; Peterson & Cudworth 1994).

The wide width of the RGB shown in the previous studies has been thought due to the different abundances of many metallic elements of RGB stars as well known in ω Centauri (Cannon & Stewart 1981). As shown in Figure 2, however, such a phenomenon does not clearly appear in the $(V - I)$ color. This implies that the wide RGB shown

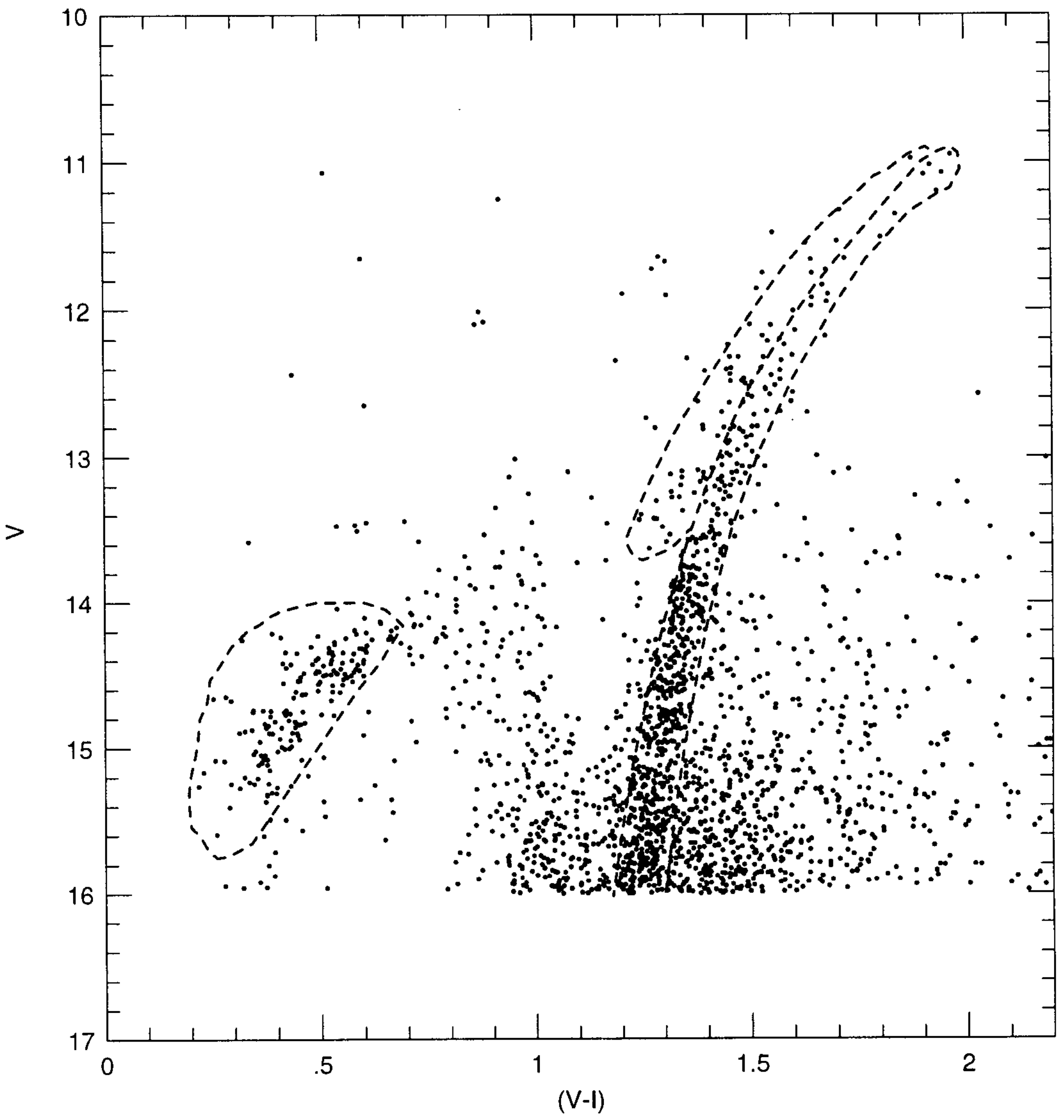

Fig. 3. The CMD for bright stars in M22. Dashed lines denote boundaries enclosing each branch stars.

in the $(V, B-V)$ CMDs could be due mainly to the B-filter whose passband includes many metallic lines, although some contribution of photomteric errors in the previous BV photometries cannot be entirely ruled out (see Figs. 2 and 3 of Côté et al. 1996).

The AGB begins to appear from $V = 13.7^m$, and it is clealy separated from the RGB up to $V = 13^m$, beyond which it approaches closely the RGB up to the RGB tip, showing no clear separation between them.

In Figure 2(a), many red stars in the right part of the RGB are field stars which are located mainly in the central region of the Galaxy. And stars which are spreaded diagonally from the left part of subgiant branch to the RR Lyrae gap in Figure 2, are severly reddened field stars (Bertelli et al. 1995; Kiraga, Paczyński & Stanek 1997). Among these bright stars near the horizontal branch (HB) level, some RR Lyrae variables are included as members of M22.

A populated BHB is well defined, extending from $V = 14.1^m$ $(I = 13.5^m)$ to $V = 15.5^m$ $(I = 15.4^m)$. It is noted that the BHB is more sharply defined in the $(I, V-I)$ CMD as seen in Figure 2(b). Stars with $(V-I) < 0.03^m$ are seen between $V = 16.5^m \sim 18^m$. At present, it is not clear whether they are sdB stars (Moehler et al. 1995) belonging to the extended BHB stars which are seen in some globular clusters such as NGC 6752 (Lee et al. 1995; Lee & Cannon 1997), M13 (Arp & Johnson 1955; Paltrinieri et al. 1998) and M15 (Durrell & Harris 1993). In the

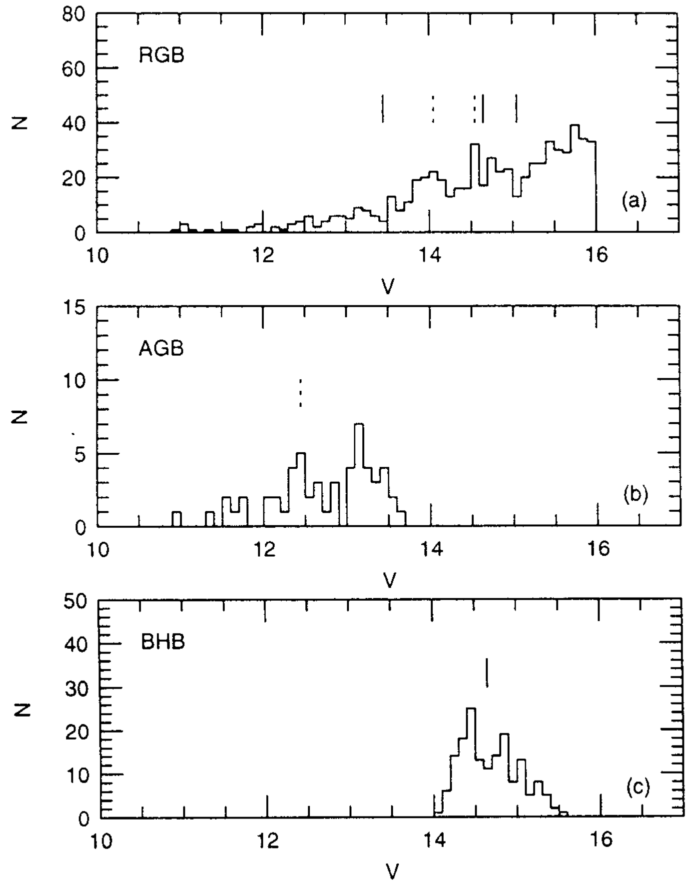

Fig. 4. (a) Differential LF for RGB stars. (b) Differential LF for AGB stars. (c) Differential LF for BHB stars. Vertical solid lines indicate the positions of deficient gaps and vertical dotted lines indicate the positions of bumps.

region redder than the red end of the RR Lyrae gap, few red HB stars are found, as reported in the previous studies.

IV. LUMINOSITY FUNCTION

In order to investigate the distributions of stars along the RGB, BHB and AGB, LFs for each branch stars are needed. In Figure 3, the RGB stars brighter than $V \approx 13.5^m$ do not show a clear boundary from the AGB stars, and so we separated the AGB and RGB into the two areas enclosed by the dashed lines considering that the RGB becomes narrower as it becomes brighter. For the BHB stars, we selected only stars brighter than $V = 16^m$ and they are enclosed by the dashed line as shown in Figure 3. The LFs for the RGB, AGB and BHB stars are shown in Figure 4 where magnitude interval was taken as 0.1^m.

There appear three deficient gaps along the RGB in Figure 4(a). The first gap appears at $V \approx 13.4^m$ ($\sim 0.8^m$ above the HB level), the second gap at $V \approx 14.7^m$ ($\sim 0.5^m$ below the HB level) and the third gap at $V \approx 15.1^m$ ($\sim 0.9^m$ below the HB level). The third gap had been shown by Alcaino (1977) and Alcaino & Liller (1983). Two bumps appear along the RGB. A relatively broad bump is seen at $V \approx 14^m$ ($\sim 0.2^m$ above the HB level) and sharp bump at $V \approx 14.6^m$. The former bump is also seen in NGC 3201 (Lee 1977a) and M55 (Lee 1977b) at the HB level and in NGC 6752 (Lee & Cannon 1997) with a peculiarly extended BHB just above the HB level.

As seen in Figure 4(b), a clear bump appears at $V \approx 12.4^m$, $\sim 1^m$ above the bottom of AGB. This bump is seen in most of globular clusters. According to the AGB models (Gingold 1974; Iben 1982), this position on the CMD corresponds to the first thermal pulsating stage during the AGB evolution.

In the LF for BHB stars, one deficient gap appears at $V = 14.7^m$ as shown in Figure 4(c) where the HB level is defined at $V = 14.15^m$ as shown by Alcaino (1977). This gap is also seen in most globular clusters with a well developed BHB such as NGC 3201 (Lee 1977a), M13 (Arp & Johnson 1955; Paltrinieri et al. 1998), M12 (Racine 1971), NGC 6752 (Lee & Cannon 1997), M55 (Lee 1977b) and M15 (Durrell & Harris 1993). According to Newell (1973) and Newell & Graham (1976), this gap corresponds to the Newell's gap 1.

V. CONCLUSION

In the $(V, B-V)$ CMDs of M22, the slope of the bright RGB is not so steep. That is, the magnitude difference between the RGB and HB read at reddening-corrected $(B-V)_o = 1.4^m$ is small as $\Delta V = 2.5^m$ (Sandage & Wallerstein 1960). This indicates that the metallicity of M22 is similar to that of M4 and M72 which have both the BHB and RHB in the CMD. M22 has, however, only the BHB and the observed metal abundance is [Fe/H] ≈ -1.68 which is less than for M4 ([Fe/H] $= -1.33$) and M72 ([Fe/H] $= -1.54$). In this point of view, M22 has been known as an anomalous globular cluster.

Since the bright RGB of M22 shows a large scatter in $(B-V)$ color, having the intrinsic width of $\Delta(B-V) = 0.18^m$, and moreover the abnormal abundances of CH, CN and Ca were reported by Norris & Freeman (1983), it has been pointed out that the RGB stars in M22 have the inhomogeneities of heavy metals as seen in ω Centauri (Cannon & Stewart 1981). But in the VI CCD photometry presented in this study, this anomalous feature does not clearly appear. That is, in the $(V, V-I)$ CMD, the intrinsic width of the bright RGB is as narrow as $\Delta(V-I) = 0.06^m$ which is one third of $\Delta(B-V)$, and the RGB slope becomes relatively steep. This result suggests that the wide width of the RGB seen in the $(V, B-V)$ CMD might be arisen from the property of B-filter whose passband includes many metallic lines. The present study also shows clearly that although there exist some inhomogeneities of heavy elements in the atmospheres of RGB stars, its photometric effect is hardly revealed particularly in the I-band, yielding the relatively sharp bright RGB in the $(V, V-I)$ CMD. This result further suggests that the effect of differential reddening (Bates et al. 1991) across the south-eastern part of M22 is not so seriously involved even in the appearance of a wide width of RGB in the $(V, B-V)$ CMD.

Along the RGB, there appear three deficient gaps ($\sim 0.8^m$ above, $\sim 0.5^m$ below and $\sim 0.9^m$ below the HB level) and two bumps ($\sim 0.2^m$ above and $\sim 0.5^m$ below the HB level). The bright bump is also seen in other globular clusters (Lee 1977a, 1977b; Fuci Pecci et al. 1990; Saviane et al. 1998; Paltrinieri et al. 1998). According to the relation of bump position with metallicity of globular clusters (Saviane et al. 1998), M22 should be a more metal-poor cluster than at least NGC 3201 (Lee 1977a) which has both the RHB and BHB. The existence of RHB stars is confirmed not to be evident in M22. Along the populated BHB, there is a distinct gap at $V = 14.7^m$. This corresponds to the Newell's gap 1 and is seen in the most of globular clusters with an extended BHB (Lee 1977a, 1977b, 1997; Durrell & Harris 1993; Paltrinieri et al. 1998; Racine 1971).

REFERENCES

Alcaino, G. 1977, A&AS, **29**, 383.
Alcaino, G., & Liller, W. 1983, AJ, **88**, 1330.
Alcaino, G., Liller, W., & Alvarado, F. 1988, AJ, **96**, 139.
Arp, H. C., & Johnson, H. L. 1955, ApJ, **122**, 171.
Arp, H. C., & Melbourne, W. E. 1959, AJ, **64**, 28.
Bates, B., Gilheany, S., & Wood, K. D. 1991, MNRAS, **252**, 600.
Bertelli, G., Bressan, A., Chiosi, C., Ng, Y. K., & Ortolani, S. 1995, A&A, **301**, 381.
Brown, J. A., & Wallerstein, G. 1992, AJ, **104**, 1818.
Butler, D. 1975, ApJ, **200**, 68.
Cannon, R. D., & Stewart, N. J. 1981, MNRAS, **195**, 15.
Canterna, R. 1975, ApJ, **200**, L63.
Carretta, E., & Gratton, R. G. 1997, A&AS, **121**, 95.
Cohen, J. G. 1981, ApJ, **247**, 869.
Côté, P., Pryor, C., McClure, R. D., Fletcher, J. M., & Hesser, J. E. 1996, AJ, **112**, 574.
Crawford, D. L., & Barnes, J. V. 1975, PASP, **87**, 65.
Crocker, D. A. 1988, AJ, **96**, 1649.

Cudworth, K. M. 1986, AJ, **92**, 348.
Durrell, P. R., & Harris, W. E. 1993, AJ, **105**, 1420.
Eggen, O. J. 1972, ApJ, **172**, 639.
Fusi Pecci, F., Ferraro, F. R., Crocker, D. A., Rood, R. T., & Buonanno, R. 1990, A&A, **238**, 95.
Gillett, F. C., Jacoby, G. H., Joyce, R. R., Cohen, J. G., Neugebauer, G., Soifer, B. T., Nakajima, T., & Mattews, K. 1989, ApJ, **338**, 862.
Gingold, R. A. 1974, ApJ, **193**, 177.
Glaspey, J. W., Demers, S., Moffat, A. F. J., & Shara, M. 1985, ApJ, **289**, 326.
Gratton, R. G. 1982, A&A, **115**, 171.
Gratton, R. G., & Ortolani, S. 1989, A&A, **211**, 41.
Harris, W. E., & van den Bergh, S. 1974, AJ, **79**, 31.
Hesser, J. E. 1976, PASP, **88**, 849.
Hesser, J. E., & Harris, G. J. H. 1979, ApJ, **234**, 513.
Hesser, J. E., Hartwick, F. D. A., & McClure, R. D. 1977, ApJS, **33**, 471.
Hertz, P., & Grindlay, J. E. 1983, ApJ, **275**, 105.
Iben, I., Jr. 1982, ApJ, **260**, 821.
Johnson, S. L., & McNamara, D. H. 1969, PASP, **81**, 415.
Kiraga, M., Paczyński, B., & Stanek, K. Z. 1997, ApJ, **485**, 611.
Landolt, A. U. 1992, AJ, **104**, 340.
Lee, K. H., Lee, S.-W., & Jeon, Y. B. 1995, J. Korean Astron. Soc., **28**, 153.
Lee, S.-W. 1977a, A&AS, **28**, 409.
Lee, S.-W. 1977b, A&AS, **29**, 1.
Lee, S.-W., & Cannon, R. D. 1997, J. Korean Astron. Soc., **30**, 135.
Lehnert, M. D., Bell, R. A., & Cohen, J. G. 1991, ApJ, **367**, 514.
Luck, R. E., 1991, in IAU Symp. **145**, *Evolution of Stars: The Photometric Abundance Connection*, ed. G. Michaud and A. Tutukov (Dordrecht: Kluwer), p. 247.
Mallia, E. A. 1976, MNRAS, **177**, 73.
Manduca, A., & Bell, R. A. 1978, ApJ, **225**, 908.
Minniti, D. 1995, A&A, **303**, 468.
Moehler, S., Heber, U., Saffer, R., & Thejll, P. 1995, BAAS, **27**, 1404.
Newell, B. 1973, ApJS, **26**, 37.
Newell, B., & Graham, J. A. 1976, ApJ, **204**, 804.
Norris, J., & Freeman, K. C. 1983, ApJ, **266**, 130.
Paltrinieri, B., Ferraro, F. R., Fusi Pecci, F., & Carretta, E. 1998, MNRAS, **293**, 434.
Peterson, C. J., & King, I. R. 1975, AJ, **80**, 427.
Peterson, R. C. 1980, ApJ, **237**, L87.
Peterson, R. C., & Cudworth, K. M. 1994, ApJ, **411**, 103.
Philip, A. G. D., & Goodman, B. M. 1975, PASP, **87**, 801.
Pilachowski, C., Leep, E. M., Wallerstein, G., & Peterson, R. C. 1982, ApJ, **263**, 187.
Pryor, C., & Meylan, G. 1993, in ASP Conf. Ser. **50**, *Structure and Dynamics of Globular Clusters*, ed. G. Meylan and S. Djorgovski (San Francisco: ASP), p. 357.
Racine, R. 1971, AJ, **76**, 331.
Reed, B. C., Hesser, J. E., & Shawl, S. J. 1988, PASP, **100**, 545.
Sandage, A., & Wallerstein, G. 1960, ApJ, **131**, 598.
Saviane, I., Piotto, G., Fagotto, F., Zaggia, S., Capaccioli, M., & Aparicio, A. 1998, A&A, **333**, 479.
Stetson, P. B., Davis, L. E., & Crabtree, D. R. 1990, in ASP Conf. Ser. **8**, *CCDs in Astromony*, ed. G. H. Jacoby (San Francisco: ASP), p. 289.
Wallerstein, G., Leep, E. M., & Oke, J. B. 1987, AJ, **93**, 1137.
Zinn, R. 1980, ApJS, **42**, 19.